Proceedings of the 35th European Safety and Reliability & the 33rd Society for Risk Analysis Europe Conference
Edited by Eirik Bjorheim Abrahamsen, Terje Aven, Frederic Bouder, Roger Flage, Marja Ylönen
 Published by Research Publishing, Singapore.
doi: 10.3850/978-981-94-3281-3_ESREL-SRA-E2025-P5050-cd

Formulation, calibration and testing of a coarse-grained heating model for urban resilience assessment

Mara Böhler, Corinna Köpke, Benjamin Lickert, Johannes Walter, Mirjam Fehling-Kaschek, Alexander Stolz

Fraunhofer Ernst-Mach-Institute, EMI, Efringen-Kirchen, Germany E-mail: Benjamin.Lickert@emi.fraunhofer.de

Climate change causes a multitude of challenges, not only for nature but also for human lifestyle. One significant consequence of climate change, expected to increasingly threaten urban resilience, is the phenomenon of heat accumulation in cities during summer heat waves. Although small-scaled countermeasures, like cooling rooms for elderly and other vulnerable people, help to dampen the worst consequences of heat waves, the whole architecture of cities needs to change to preserve the general quality of life. An increase of urban vegetation or the installation of large water basins represent typical procedures at this point. Given that the implementation of such interventions costs time and money, simulation tools are needed to predict and compare the benefits of different implementation strategies in order to enable an effective increase of the urban resilience against heat. Still, established simulation frameworks, like PALM and ENVI-met, need elaborate input and are computationally demanding making it complicated and tedious to apply them to whole cities and multiple different scenarios.
Addressing this complexity problem, this contribution presents a model framework which predicts the evolution of the air temperature in a coarse-grained manner based on large-scale factors, like the atmospheric temperature, sun radiation and local heat diffusion. The framework can be run on conventional laptops/PCs predicting a few days of temperature evolution within seconds to minutes. It will be shown how ESA satellite data is used to transfer local characteristics of the (urban) environment under study into a model grid of numerous small tiles. Types like "built-up", "tree cover" or "water" are assigned to the tiles, each type is characterized by a unique parameter set representing the response to incoming heat. Using an exemplary model of Basel, Switzerland, it will be shown how those parameters are calibrated and the performance of the model is assessed.

Keywords: Resilience Assessment, Modelling, Simulation, Urban Heating, Mitigation, Meteorological Data

1. Introduction

According to NASA, the summer temperatures are increasing since recording began. 2023 marked the hottest year on record since 1880 (Fox & Keck, 2023). This increase in temperature is particularly pronounced in urban areas, where the Urban Heat Island (UHI) effect leads to higher temperatures compared to rural regions (Oke, 1982; Yow, 2007). The UHI effect is primarily caused by differences in land use, such as the presence of buildings and streets, which disrupt the natural energy and water balance, alter wind patterns, and raise temperature levels (Oke, 1982). The higher temperatures pose significant challenges in naturally warmer regions and seasons, jeopardizing the health of urban residents. Research indicates that the occurrence and intensity of heat-related health issues, including heat exhaustion, heat stroke, and dehydration, are on the rise (Ballester et al., 2023). Vulnerable groups, such as the elderly, young children, and individuals with pre-existing health conditions, face greater risks in areas affected by UHI effect (Ward et al., 2016). Consequently, it is essential for cities to enhance their resilience to heat during warmer periods to safeguard their populations from heat-related dangers. Understanding the evolution of urban climates, identifying the most impacted areas, and exploring strategies to mitigate urban heat are crucial steps. For instance, increasing green spaces like parks or incorporating water features can help regulate temperatures (Gunawardena et al., 2017). Additionally, modifying the properties of construction materials used for roads and roofs can also contribute to limiting the UHI effect (Shamsaei et al., 2022). However, cities differ significantly in their structures and local weather patterns, which means that the most

suitable mitigation strategies can vary greatly from one city to another.

To effectively plan, evaluate and compare different mitigation strategies, city planners can utilize urban climate models that simulate temperature changes, pollution dispersion, and airflow in the targeted areas. This approach offers advantages in terms of saving time and reducing costs, as it eliminates the need to test each mitigation strategy sequentially in real-world settings. These climate models differ in terms of temporal and spatial resolution, as well as in their complexity (Vurro & Carlucci, 2024). For instance, models like ENVI-met (*ENVI-Met*, 2024) and PALM (Leibniz Universität Hannover, 2024) require substantial computational power and time to operate. This challenge is exacerbated by the need for highly detailed input data to construct their (three-dimensional) models, which is often not readily available. In consequence, those models are typically applied on micro- or meso-scale, i.e., for individual buildings with direct surrounding or city districts, but it is difficult to use them for entire metropolitan areas, let alone for a study encompassing several cities.

For this application case, a low-input two-dimensional urban heat model is introduced in the following, see Fig. 1 for a visualization of the presented work. This model, called EMIHeat, is able to cover large geographical regions based on limited, openly available input data. EMIHeat divides the area to be analyzed into squares ('tiles') to which different land types and thus properties are assigned. The assignment is done by determining the dominant land type of the tile based on satellite data information. The temperature evolving over time is calculated for each tile, considering solar radiation and heat exchange at the surface as well as with the atmosphere. The major advantage of this model is that, by projecting the study area to a two-dimensional model, as well as by simplifying the calculation, the computational effort and the needed input information are reduced, so that the associated ease of use is maximized. As exemplary application, this paper presents simulation results for a section of the city of Basel in Switzerland.

2. Background and Model Framework

The urban climate is very complex and influenced by many factors such as the geographical location, the meteorology including wind, clouds and humidity, but also the city structure. Cities can have various sizes, different shares and compositions of vegetation and different building densities, alignments, and heights. In combination, this has an influence on the reaction to solar radiation that reaches the surface representing the main contributor to the urban heat (Oke et al., 2017). The albedo with values between 0 and 1 describes the ability of a material to reflect incoming radiation. In general the albedo for urban materials such as asphalt or concrete is low. Newly build asphalt, for example, has an albedo of 0.05 (Shamsaei et al., 2022). Moreover, due to the high heat capacities of urban materials, they often store a significant amount of energy in form of sensible heat over the day and release this energy over the night, reducing the capability of the city to cool down (Oke et al., 2017). Sensible heat describes at this point the energy that results in a direct temperature change of any material. Additionally, by replacing natural surfaces with asphalt or concrete, the evaporation from soil and plants is reduced. The associated energy that is absorbed or released by a phase change is often called latent heat flux. Its reduction has a relevant influence on the urban climate as this possibility of cooling is reduced (Oke et al., 2017; Winbourne et al., 2020). Furthermore, the heat which is generated by human activities such as cooling and heating of buildings or the use of transportation, called anthropogenic heat, has also an effect on the urban temperature.

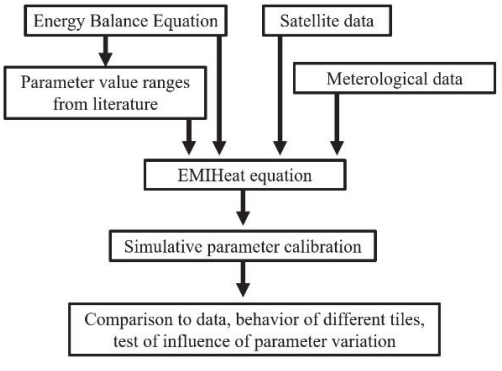

Fig. 1: Visualization of the research presented in this paper.

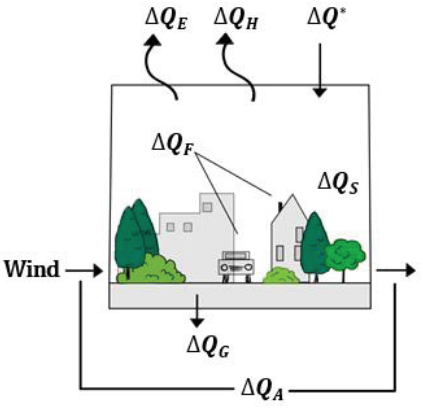

Fig. 2: Schematic illustration of the Energy Balance for an "urban air volume". The drawing is based on (Oke et al. 2017).

2.1. *Energy Balance Equation*

One approach to describe the urban climate is to formulate a balance equation, typically called the Surface Energy Balance (SEB), which in its original form describes the energy exchange of a surface, based on the latent (ΔQ_E), sensible (ΔQ_H), and ground (ΔQ_G) heat flux as well as the net radiation (ΔQ^*) (Oke, 1982). When extending the investigated system to some sort of "urban air volume", the anthropogenic heat (ΔQ_F), as well as the change of stored energy (ΔQ_S) and the change of windborne energy transport (ΔQ_A) need to be included (Oke et al., 2017). In total, this leads to Eq. (1). ΔQ_S represents the heat energy which leads to a temperature change of the "urban air volume" under investigation.

$$\Delta Q_S = \Delta Q^* + \Delta Q_H + \Delta Q_F + \Delta Q_E + \Delta Q_G + \Delta Q_A \quad (1)$$

Please note that the time dependence of all terms of Eq. (1) is omitted for the sake of readability, the direction of the energy flows, i.e., whether the different flows have a cooling or a heating influence, can change over the day, as indicated by their sign. Positive values signify energy gained by the "urban air volume" (heating), while negative values indicate that energy is lost (cooling). A graphical illustration of the Energy Balance of the "urban air volume" can be found in Fig. 2.

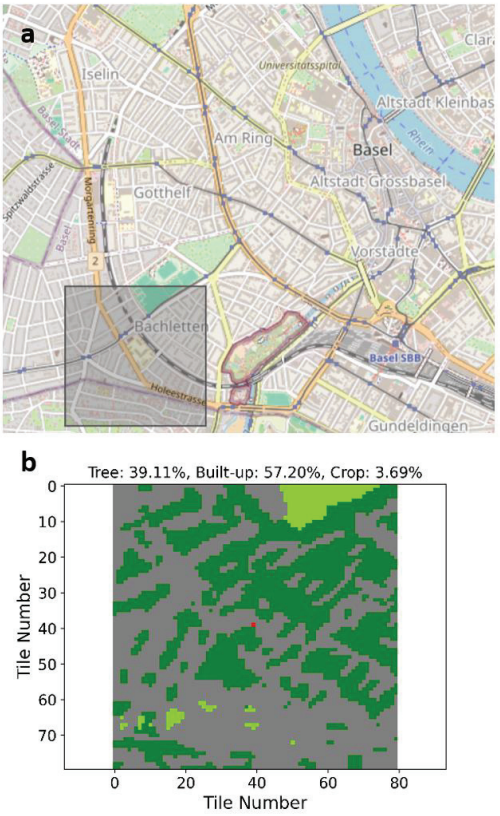

Fig 3: (a) Map of Basel, the highlighted area (grey) represents the section investigated in this work. (b) Tile model for the considered part of Basel (centred at longitude, latitude = 7.568918, 47.546944). The colour represents the land type: grey: built-up; dark green: tree cover; light green: grassland; red: measurement point (Meteoblue, see below).

2.2. *The EMIHeat Model*

EMIHeat depicts the area under study as a two-dimensional system of connected rectangles, called "tiles" in the following, see Fig. 3 b. Using for example satellite data, see Section 3.1, each of these tiles gets a "land type" assigned. Currently, EMIHeat differentiates four different land types: built-up, tree cover, grassland and water, simplifying a convention of the ESA (European Space Agency, 2024).

Based on meteorological input data, e.g., the evolution of incoming radiation, see Section 3.2, EMIHeat then calculates the temperature evolution in discrete timesteps Δt. Here, the temperature trajectory for tile i is calculated using Eq. (2).

$$T_i(t) = T_i(t - \Delta t) + \Delta T(t) \quad (2)$$

with $T_i(t)$ being the current temperature of tile i at time t, $T_i(t - \Delta t)$ being the temperature of the previous timestep and the temperature change $\Delta T(t)$ depending on several contributions, which will be discussed in the following.

To derive $\Delta T(t)$, the Energy Balance Eq. (1) is recalled and some simplifications are made. First, the ground heat flux, which can be described by $\Delta Q_G(t) = k \frac{\Delta T_G(t)}{\Delta z} \Delta t$ with k being the associated ground conductivity, $\Delta T_G(t)$ the temperature difference between ground and air at time t, and Δz the vertical distance, is assumed to be negligible. This means that it is assumed that the ground follows the temperature evolution of the air ($\Delta T_G(t) = 0$), i.e. $\Delta Q_G(t) = 0$. Second, the current version of EMIHeat neglects the contributions of $\Delta Q_E(t)$ and $\Delta Q_F(t)$, since it is assumed that both energies play a minor role compared to the other terms. Finally, the wind-dependent contribution $\Delta Q_A(t)$ is neglected, since this depends on a correct transfer of three-dimensional information (wind depends on heights of, e.g. buildings) to the two-dimensional model which exceeds the scope of this work.

As written above the term of the energy storage $\Delta Q_S(t)$ describes the heat energy stored by the urban air volume at time t and is directly related to the temperature change of the air within the element. Inserting $\Delta Q_S(t) = \rho_i \, c_i \, V \Delta T(t)$, where c_i (J Kg^{-1} K^{-1}) is the specific heat capacity, ρ_i (Kg m^{-3}) the density and V (m^3), the equation can be transformed to Eq. (3).

$$\Delta T(t) = \frac{1}{\rho c V} (\Delta Q^*(t) - \Delta Q_{H,1}(t) - \Delta Q_{H,2}(t)) \quad (3)$$

Here, the remaining terms can be inserted. Regarding the radiation contribution $\Delta Q^*(t)$, only the short-wave radiation is currently included into EMIHeat, as the net incoming short-wave radiation is expected to be larger compared to the net longwave radiation. Thus $\Delta Q^*(t)$ only depends on the (tile-type-dependent) albedo α_i, the incoming shortwave radiation $R_S(t)$, the tile area A and the time step Δt.

$$\Delta Q^*(t) = (1 - \alpha_i) \, R_S(t) \, \Delta t \, A \quad (4)$$

The sensible heat flux $\Delta Q_H(t)$, is separated into two terms that differentiate the directions of heat transfer. The first term $\Delta Q_{H,1}(t)$, covers the (vertical) heat transfer to the atmosphere and the second term $\Delta Q_{H,2}(t)$ represents the (horizontal) heat exchange with neighbouring tiles. $\Delta Q_{H,1}(t)$ dependents on the temperature difference between the atmosphere and the tile ($T_{atm}(t) - T_i(t)$) and is multiplied by the area A (m^2) of the tile. The tile-dependent heat transfer coefficient h_i (W m^{-2} K^{-1}) is introduced to describe how effectively heat is transferred by the different tile types. The formula for $\Delta Q_{H,1}(t)$ is given by Eq. (5).

$$\Delta Q_{H,1}(t) = h_i \, A \left(T_{atm}(t) - T_i(t)\right) \Delta t \quad (5)$$

The heat transfer $\Delta Q_{H,2}(t)$ with neighbouring tiles j is given by Eq. (6).

$$\Delta Q_{H,2}(t) = \sum_{j=1}^{4} k_{ex,i,j} \left(T_i(t) - T_j(t)\right) L \, \Delta t \quad (6)$$

with L representing the side length of the tiles. The conductivity $k_{ex,i,j}$ (W m^{-1} K^{-1}), which defines the four temperature exchanges with the neighbouring tiles, is calculated following function Eq. (7) with k_i being dependent on the tile type.

$$k_{ex,i,j} = \frac{k_i k_j}{k_i + k_j} \quad (7)$$

Inserting Eq. (3) to (7) into Eq. (2) leads to the temperature propagation equation of EMIHeat.

3. Tile Model of Basel and Data Source

As explained in Section 2.2, EMIHeat uses geographical input information, as provided by satellite data, to assign the land types for the two-dimensional tile model as well as data regarding the meteorological conditions, i.e., the atmospheric temperature as well as the shortwave radiation. The following sections explain the data sources used to generate the model results presented in section 4.

3.1. *Satellite Data*

To assign the land types to the tiles of the area of interest, satellite data from ESA is used

(European Space Agency, 2024). The information for the area was extracted via a Python program and the land types provided by ESA were reassigned to the four land types defined in EMIHeat. While the NASA provides the data in form of a GeoTIFF, the tile model of EMIHeat is saved in csv format. Fig. 3 provides a visualization of the resulting tile model for a part of Basel. The area has a share of 57.20 % built-up, 39.11 % tree cover and 3.69 % grass land. It consists of 80x80 tiles (800x800 m), where the measurement point of the temperature (longitude, latitude = 7.568918, 47.546944) is in the centre.

3.2. *Meteorological Data*

For this work the meteorological data was taken from Meteoblue (Meteoblue, 2024), which provides the atmospheric temperature at 850 m, as well as the incoming shortwave radiation for one location (longitude, latitude = 7.568918, 47.546944) in Basel for free. In addition, the measured temperature at 2 m height is provided and was used for evaluating the performance of EMIHeat. The inspected time period is August 2022, the time resolution is $\Delta t = 1$ h.

4. Parameter Calibration

Having specified the tile model as well as the data source for metrological data and the considered time period, the next section considers the selection of model parameters.

4.1. *Literature Research*

EMIHeat distinguishes four different tile types (built-up, tree cover, grassland and water) each having five parameters (albedo α_i, conductivity k_i, density ρ_i, heat coefficient h_i and specific heat capacity c_i). Specific values (or at least value ranges) for some of these parameters can be found in literature. First, there are value ranges for albedos of urban as well as natural environments. Nevertheless, these albedo values vary with the geographical location as well as with the specific composition of the material, for example the albedo of trees depends on the tree type and the size and shape of the crone. This makes it challenging to assign one value to the vegetation land type. Similar difficulties were found for built-up, grassland and water.

Table 1: Calibration results for the parameters of the different land types used in EMIHeat. Water was calibrated inspecting another part of Basel (not shown in this paper).

	Built-up	**Grassland**	**Tree Cover**	**Water**
Albedo	0.21	0.16	0.15	0.1
Conductivity	0.94	0.41	0.05	0.689
Density	523	200	150	170
Heat Coefficient	28	43	50	40
Specific Heat Capacity	1250	3000	3000	4200

Additionally, specific heat capacity values and conductivities can be found in the literature but, again, local conditions play a major role, making it necessary to do some calibration via tests of the simulation. Finding literature values for density and heat coefficient turned out to be challenging, in consequence, they were set by hand for this paper.

4.2. *Calibrating the Parameters*

To determine the optimal values for the model parameters, simulative tests were performed investigating the value ranges found in literature for albedo, specific heat capacity and conductivity. For the heat coefficient as well as the density plausible value ranges, i.e., value ranges where test calculations of Eq. (3) and Eq. (5) yielded realistic numbers, were set by hand and the best values were chosen by simulative testing. The optimal parameter values can be found in Table 1. When testing, it was found that currently the conductivity has only a minor influence on the temperature prediction of EMIHeat and thus the calibration results need to be treated with caution. In addition, there is a significant correlation between the influences of density and specific heat capacity, i.e., changes in one parameter can be compensated by changes of the other one. Given that both parameters enter the model equation as product, this observation is not surprising.

5. Simulation Results

Having calibrated the model parameters, this section presents the simulation results of EMIHeat. Section 5.1 compares the temperature

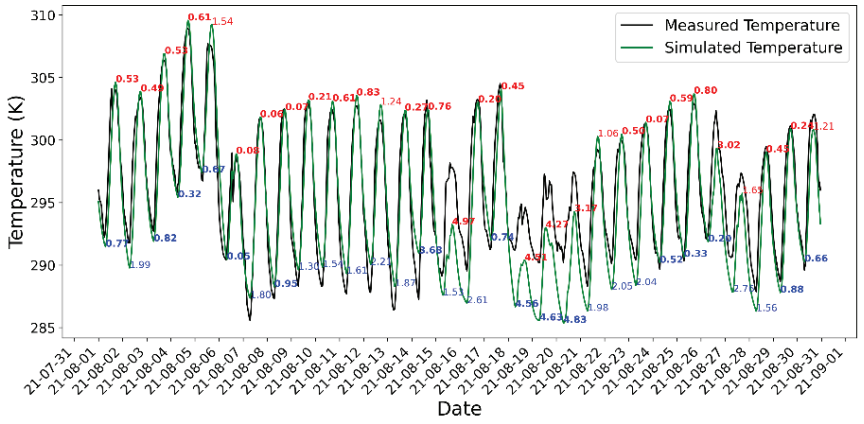

Fig. 4: Measured and simulated temperatures from EMIHeat for Basel in August 2022. The mean absolute error of the two curves is 1.92 K.

curve of EMIHeat at the measurement point to the provided data from meteoblue (tile type built-up). Section 5.2 compares the development of the different tile temperatures and section 5.3 presents a simulation of an exemplary UHI mitigation measure.

5.1. *Performance in Comparison to Data*

EMIHeat can simulate the temperature at the measurement point with a mean absolute error of 1.92 K for August 2022 very well, see Fig. 4. Especially the maxima are well reproduced (red numbers show the deviations between data and simulation at maxima). However, there are several days where the simulated temperature deviates from the measured temperature, for example the 16th and 19th and 20th August.

5.2. *Comparison Behaviour of Tile Types*

Fig. 5 shows the individual tile temperature over time. We see that the tiles behave realistically, as built-up tiles have higher temperatures over the day, compared to grassland and tree cover However, the exact temperature difference between the built-up and the tree cover might be smaller or larger and must be calibrated in future using several measurement points available in close proximity but at different tile types.

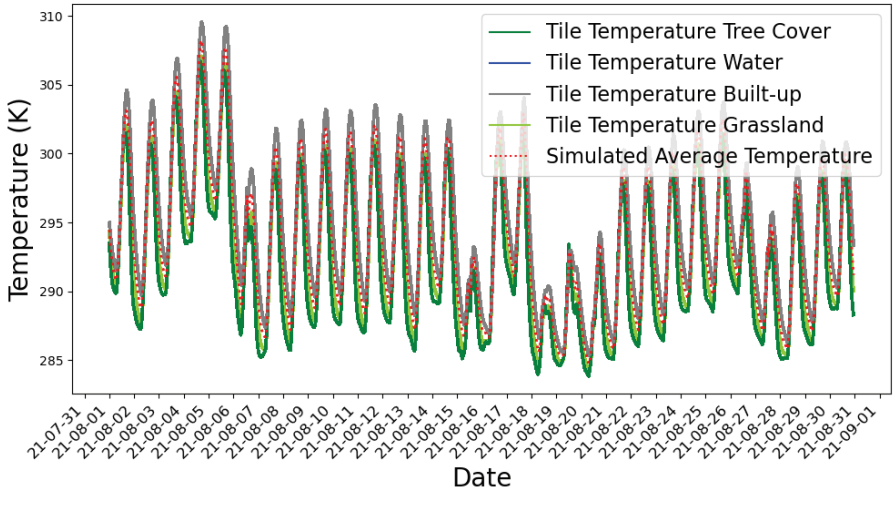

Fig. 5: Simulated tile temperatures for each tile. Here the colour indicates the tile type.

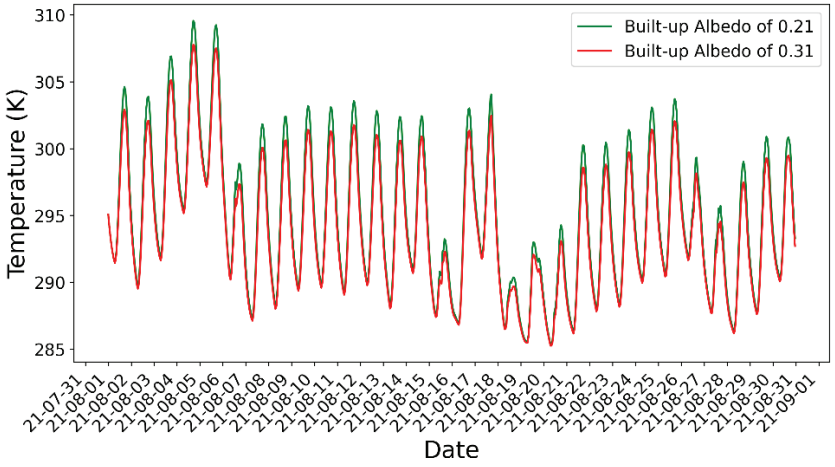

Fig. 6: Simulated temperature for Basel with different built-up albedo value.

5.3. *Simulation of Heat Mitigation*

To mitigate the UHI effect, an increase of the reflection capabilities of streets and house roofs are a promising strategy. In terms of the EMIHeat parameters, this measure translates to an increase of the albedo of built-up tiles, indicating that a larger share of solar radiation is reflected. Fig 6 compares the results of EMIHeat for an albedo of 0.31 to the default value (0.21). It can be seen that the temperature peaks are reduced up to 1.75 K over the day. However, no changes in temperature due to the albedo can be found at night.

6. Conclusions and Outlook

In this work the EMIHeat model framework was introduced, a parameter calibration was shown and exemplary simulation results for a model of Basel were presented. We have seen that the model can reproduce the temperature for Basel reasonably well, has different behaviours for different tile types and shows plausible reactions to changes of model parameters. When increasing the albedo value for built-up, the daily highs of the temperature trajectory were reduced. Still, this example only represents a somewhat abstracted heat mitigation measure; the in-depth modeling and comparison of different heat mitigation options remain for future work.

EMIHeat represents an alternative to established (three-dimensional) modeling frameworks, like ENVI-met or PALM, which can reach their limits when investigating larger geographical regions. In terms of raw computational power and required input data, EMIHeat is much less demanding than those frameworks; however, the downside is that the precision of the modeling results is not as high. Therefore, EMIHeat is useful when model results are needed to inspect and compare whole cities, while frameworks like ENVI-met or PALM can be used for applications on a smaller scale with sufficiently available data.

Regarding limitations, the presented calibration was based on a single temperature measurement point and the temperature exchange between neighbouring tiles only plays a minor role with the current parameter set. Thus, in future work it is planned to have several measurement points on different land types within one city, so that first, the parameter sets of each tile type could be calibrated individually in small, separated tile models. In a second step the exchange between the different tiles based on $\Delta Q_{H,2}$ is calibrated using a larger tile model which includes all measurement points. Furthermore, there are still some deviations between the simulated temperature and the data which demand further investigation. In can be expected that important meteorological information is currently not

sufficiently incorporated, such as the presence of clouds and wind. Moreover, the relevance of latent heat and anthropogenic heat needs to be closer investigated. Additionally, this work investigates the measured temperature and not the physiological temperature which is felt by the individual. Since this is ultimately the critical parameter for the UHI effect, future work should investigate how EMIHeat could account for the physiological temperature.

Acknowledgement

This work is funded by the project No. 101121210 "CityNature-Based Solutions Integration to Local Urban Infrastructure Protection for a Climate Resilient Society" (NBSINFRA) from the European Union's Horizon 2022 program. Views and opinions expressed are however those of the author(s) only and do not necessarily reflect those of the European Union or REA. Neither the European Union nor the granting authority can be held responsible for them.
Additionally, this work was partially funded by the Eva Mayr Stihl Foundation.
The authors express their sincere gratitude to meteoblue for providing the weather data for Basel used in this research. The comprehensive dataset significantly contributed to this study.

References

Ballester, J., Quijal-Zamorano, M., Méndez Turrubiates, R. F., Pegenaute, F., Herrmann, F. R., Robine, J. M., Basagaña, X., Tonne, C., Antó, J. M., and Achebak, H. (2023). Heat-related mortality in Europe during the summer of 2022. *Nature Medicine*, *29*(7), 1857–1866. https://doi.org/10.1038/s41591-023-02419-z

ENVI-met. (2024, November 22). https://envi-met.com/de/

European Space Agency. (2024, November 22). *ESA World Cover*. https://esa-worldcover.org/en

Fox, K. and Keck, A. (2023). *NASA Announces Summer 2023 Hottest on Record.* NASA. https://www.nasa.gov/news-release/nasa-announces-summer-2023-hottest-on-record

Gunawardena, K. R., Wells, M. J., and Kershaw, T. (2017). Utilising green and bluespace to mitigate urban heat island intensity. *The Science of the Total Environment*, *584-585*, 1040–1055. https://doi.org/10.1016/j.scitotenv.2017.01.158

Leibniz Universität Hannover. (2024, November 24) *PALM-4U* [Computer software]. https://palm.muk.uni-hannover.de/trac/wiki/palm4u

Meteoblue. (2024, November 24). *Download Historischer Wetterdaten*. https://www.meteoblue.com/de/wetter/archive/export

Oke, T. R. (1982). The energetic basis of the urban heat island. *Quarterly Journal of the Royal Meteorological Society*, *108*(455), 1–24. https://doi.org/10.1002/qj.49710845502

Oke, T. R., Mills, G., Christen, A., and Voogt, J. A. (2017). *Urban climates*. Cambridge University Press.

Shamsaei, M., Carter, A., and Vaillancourt, M. (2022). A review on the heat transfer in asphalt pavements and urban heat island mitigation methods. *Construction and Building Materials*, *359*, 129350. https://doi.org/10.1016/j.conbuildmat.2022.129350

Vurro, G., and Carlucci, S. (2024). Contrasting the features and functionalities of urban microclimate simulation tools. *Energy and Buildings*, *311*, 114042. https://doi.org/10.1016/j.enbuild.2024.114042

Ward, K., Lauf, S., Kleinschmit, B., and Endlicher, W. (2016). Heat waves and urban heat islands in Europe: A review of relevant drivers. *The Science of the Total Environment*, *569-570*, 527–539. https://doi.org/10.1016/j.scitotenv.2016.06.119

Winbourne, J. B., Jones, T. S., Garvey, S. M., Harrison, J. L., Wang, L., Li, D., Templer, P. H., and Hutyra, L. R. (2020). Tree Transpiration and Urban Temperatures: Current Understanding, Implications, and Future Research Directions. *BioScience*, *70*(7), 576–588. https://doi.org/10.1093/biosci/biaa055

Yow, D. M. (2007). Urban Heat Islands: Observations, Impacts, and Adaptation. *Geography Compass*, *1*(6), 1227–1251. https://doi.org/10.1111/j.1749-8198.2007.00063.x